International Journal of Metallurgical Engineering 2013, 2(2): 230-237
DOI: 10.5923/j.ijmee.20130202.15

Identifying Boron Distribution in a Nb-B Containing Structural Steel

Balbir Singh*, Gadadhar Sahoo

R&D Centre for Iron and Steel, Steel Authority of India Limited Ranchi, 834002, India

Abstract The C-Mn-Nb-B steel, which was made in LD converter and subsequently rolled to 8 mm diameter wire rods, was used as experimental material to identify boron distribution in as-rolled state. When examined under optical microscope, the steel was found to have polygonal ferrite with 10-15% degenerated pearlite in the microstructure. Being boron as a lower atomic number element, its presence at different locations was identified by employing Auger Electron Spectroscopy. During the study, elemental distribution spectra were obtained at the grain boundary, within ferrite grain and the pearlitic regions. On superimposing these spectra at the optical image, it was revealed that boron rich compounds were present in the pearlitic regions as well as at grain boundaries. In order to understand the kinetics of boron segregation and the type of precipitates at different locations, differential thermal analysis (DTA) was carried out on powder samples of the steel for which transformation temperatures were calculated through empirical relationships. During DTA study, enthalpy and latent heat were calculated, which helped in inferring that $M_{23}(CB)_6$ precipitate is the most probable boron compound present at the grain boundaries.

Keywords Boron Distribution, Hardening, Precipitation, Structural Steel

1. Introduction

Boron is added to structural steels to improve their hardenability and is effective when added in very small amounts; the optimum being in the range of 5 to 40 ppm. Since it enhances the hardenability effect of other alloying elements, it is called alloy intensifier. It has been found to be very effective when added to low carbon alloy steels, although beneficial effect is reduced at higher carbon contents. The largest effect of boron on hardenability occurs at carbon content of about 0.10 wt.%. In addition to its beneficial effects boron appears to be detrimental to low temperature toughness properties of steels.

The mechanism through which B additions enhance hardenability needs to be understood as its enunciation may greatly help in understanding the different effects, its additions produce. Despite a relatively larger atomic size B dissolves interstitially in steels. Therefore, B atoms have an automatic tendency to migrate to open spaces such as prior austenite grain boundaries to reduce strain. Due to this they temporarily block the nucleation of equilibrium transformation products - a pre-requisite so important to enhancing hardenability in general (both the bainitic and martensitic hardenability). As the steel is being continuously cooled the final microstructure to form would thus either be bainite or martensite depending upon the alloy design. Boron is detrimental to ambient and low temperature toughness because of the embrittling effect of B atoms present along the prior austenite grain boundaries. Another feature arising out of the presence of boron in steels is that banded structure is produced. This also has an adverse effect on toughness. It is for this reason that it is often suggested that B addition would prove most efficient when added to a low carbon iron base as the embrittling effect of higher carbon content is at a minimum.

Some studies[1] have demonstrated that in Nb containing B treated steels, Nb also segregates temporarily at prior austenite grain boundaries. Thus, both the atoms when present at austenite grain boundaries retard the nucleation and development of new grains of equilibrium transformation product takes place[2]. Depending upon the effects of these two atoms on grain boundary energy and on the velocity of moving boundaries it was observed experimentally that their retarding effect on recrystallisation is more when added jointly compared to their separate effects[3]. When added in combination, Nb and B have a synergistic effect on the recrystallisation kinetics of austenite which has been attributed to the formation of (Nb,B) complexes at the newly formed grain boundaries. This increases the solute drag force of Nb atoms and in turn, decreases the boundary velocity and slows down the recrystallisation kinetics of B modified Nb containing steels. In an alloy similar to the one under study, Tomehiro et al.[4],

* Corresponding author:
bsingh@sail-rdcis.com (Balbir Singh)
Published online at http://journal.sapub.org/ijmee

however, observed the recrystallisation temperature of about 980°C. The studies have also been confirmed that presence of solutes like Nb and B in the austenite retards austenite grain growth even after recrystallisation. This directly influences the kinetics of austenite to ferrite transformation when steels are cooled continuously below Ar3 temperature.

In view of the above mentioned segregation patterns of Nb and B atoms, present study has been carried out to identify experimentally the distrution of their compounds at various locations in a structural steel. For this purpose the microstructure of the as-hot-rolled Nb-B containing steel was studied under optical microscope and Auger Electron Spectroscope. The study was supported by differential thermal analysis and empirical calculation of critical/ transformation temperatures.

2. Experimental Material

The present study was conducted on specimens drawn from 8 mm diameter wire rods of C-Mn-Nb-B steel. Prior to hot rolling, the steel was made in LD converter and cast into ingots for further rolling to 85 mm square billets in continuous billet mill. After rolling the billets were cut to 12 meter standard length and allowed to cool in cooling bed. The billets prior to being further rolled in wire rod mill were charged into the reheating furnace wherein a temperature of 1170°C was maintained at the front end and 1220°C at the back end. After soaking for 1-1½ hour, the billets were rolled to 8 mm diameter wire rods with a cumulative reduction of about 99 %. Rolling was initiated in the range of 1000-1150°C and completed in 8 passes to attain a finishing temperature of 950-1000°C. Just after finish rolling the wire rods were coiled and allowed to cool on hook conveyors. Samples for various tests were taken after the coils had cooled to room temperature. The chemical composition of the rolled product was analysed as given in Table 1.

Table 1. Chemical composition of microalloyed steel wire rod

C	0.13	S	0.025
Mn	1.05	P	0.036
Si	0.05	B	0.004
Nb	0.023	N	0.0070
Al	0.04	-	-

The mechanical properties (hardness and tensile strength) of the product conformed to ISO:898-I specification, which are presented in Table 2.

Table 2. Mechanical properties of as-hot-rolled microalloyed steel wire rod

Yield Strength	360 MPa
Ultimate Tensile Strength	550 MPa
Uniform Elongation	17.4 %
Total Elongation	35 %
Reduction in Area	70 %
Hardnes (Hv20)	189

3. Experimental Procedure

3.1. Optical Metallography

Optical metallography was carried out on 8 mm diameter as-rolled specimens. About 10 mm long pecimens were cut in transverse direction, ground and polished in usual manner on amery paper of grits up to 600. Final polishing was done on a wheel cloth with 0.1μ alumina solution as abrasive. After polishing, the specimen were rinsed in soap solution thoroughly and dried before further etching with freshly prepared 2% nital solution. The specimens thus prepared, were observed under Neophot-30 optical microscope and microstructures photographed.

3.2. Auger Electron Spectroscopy

The experimental steel was also investigated under Auger Electron Spectroscope (AES) to identify locations of B segregation. For this study about 2mm thick disc specimens were cut from 8mm diameter wire rod and polished in the usual manner. The specimens were carefully etched with freshly prepared 2% nital solution and subsequently cleaned in acetone by an ultrasonic cleaner. After drying, the freshly prepared specimen was loaded into the vacuum chamber of AES maintained at a pressure of $1.8x10^{-6}$ Pa. The specimen was exposed to primary electron beam at an accelerating voltage of 10 kV and primary electron beam current of around 10^{-7} Amps.

Segregation behaviour of various elements present in the alloy was studied by selecting different locations, such as pearlite-ferrite grain boundary, ferrite-ferrite grain boundary, within pearlitic regions and ferrite grains. During the experiment 10 sweeps were taken at each location and the average concentration calculated through dedicated computer software. Kinetic energy versus Intensity plots were obtained on X-Y recorder through the same software. For each location relative atomic concentrations of all detectable elements were determined based on the peak height after correcting for sensitivity (5).

3.3. Differential Thermal Analysis

The Differential Thermal Analysis (DTA) was conducted on the microalloyed steel wire rods on NETZSCH Simultaneous Thermal Analyser STA-409 system. About 45 mg steel sample was used in powder form which was heated in air at a controlled rate in dry alumina crucible. For this study Kaolin was used as a reference.

A heating rate of 10°C/minute was selected during the test. The start temperature for the alloy was 21°C while end temperature was set to 1200°C. The sampling time, the acquisition rate and the total time taken for the test were 3 seconds, 2 points/°K and 2 hours 6 minutes, respectively. Range for both the DTA and the DDTA were fixed at 200 °V. During an experiment, data were recorded continuously and analysed by NETZSCH DATA ACQUISITION SYSTEM. The DTA and DDTA values were plotted against temperature or time through the acquisition system itself.

3.4. Calculated Transformation Temperatures

Using the empirical relationships proposed by Andrews[6], valid for low carbon and medium carbon structural steels, the critical / transformation temperatures were worked out as follows:

Ac_1 (°C) = 723 -10.7Mn -16.9Ni +29.7Si +16.9Cr +290As +6.38 W

Ac_3 (°C) = 910 -203C1/2 -15.2Ni +44.7Si +104V +31.5Mo +13.1W

M_S (°C) = 512-453C+217(C)2-71.5(C) (Mn) -67.6(C)(Cr)-16.9Ni+15Cr-9.5Mo

M_{10}(°C) = Ms - 10 [error ± 3]

M_{50}(°C) = Ms - 47 [error ± 6]

M_{90}(°C) = Ms - 103 [error ± 12]

M_f (°C) = Ms - 215 [error ± 15]

Substituting for the elements present in the experimental steel, critical/ transformation temperatures were estimated to be:

Ac_1 = 713°C, Ac_3 = 839°C

M_s = 447°C, M_{10} = 437°C

M_{50} = 400°C, M_{90} = 344°C

M_f = 232°C

4. Results

4.1. Optical Microscopy

Representative optical photomicrograph of as-rolled wire rod is depicted in Fig.1. The figure revealed that microstructure of experimental steel comprised polygonal ferrite and pearlite. Volume fraction of pearlite, as measured at 10 different locations on the specimen, varied between 12 to 15 percent. The average ferrite grain size measured using the line intersection method was found to be ~12 µm. It is also seen from the figure that the ferrite had a mixed grain structure with about 25% of the grains being finer and in the size range of 8-10µm. Pearlite in most locations was non-lamellar and comprised degenerated morphology.

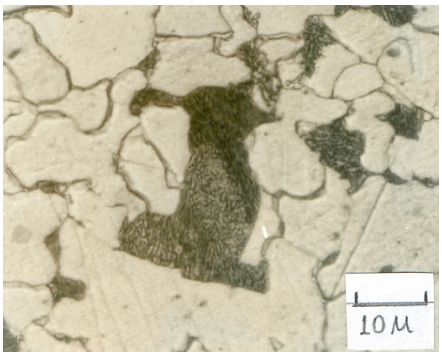

Figure 1. Microstructure of Nb-B steel

4.2. Auger Electron Spectroscopy

Auger electron spectroscopic maps presented in Figs. 2 (a & b) showed that boron rich regions existed in the steel microstructure. On comparing this map with the optical microphotograph it was revealed that the boron rich pockets existed within the pearlitic colonies. Besides this, boron was also found segregated along the grain boundaries. Line scan of boron duly supports these observations (Fig.3). Auger spectra taken at ferrite-pearlite interface (Fig.4) showed a feeble B-intensity peak at 179 ev kinetic energy. Before taking the spectra, the specimen was argon etched for three minutes to remove any adsorbed oxygen within the surface. Ion current was maintained as 20 mA at an accelerating voltage of 3 kV. Sample tilt was kept – 40° and aperture size was medium. Elemental distribution spectra obtained inside the ferrite grains (Fig.5) did not show even a feeble peak of B at 179ev kinetic energy, thereby confirming its absence at this location.

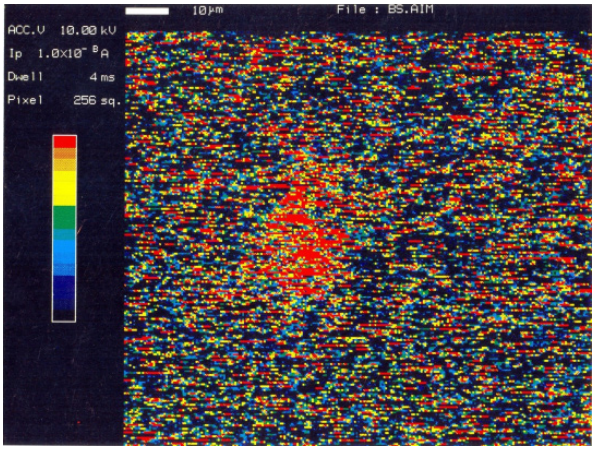

Figure 2(a). AES map showing B distribution

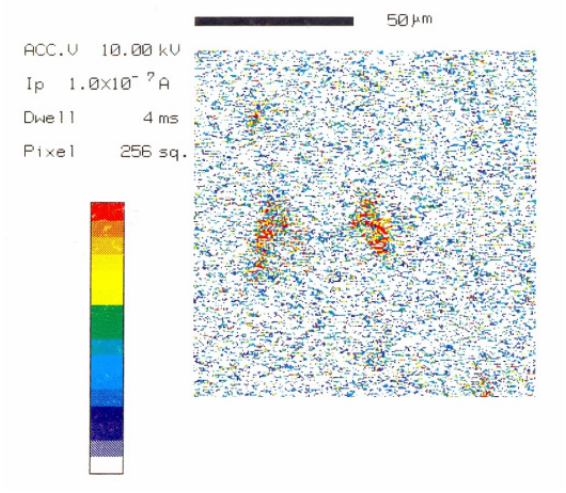

Figure 2(b). AES map showing B distribution

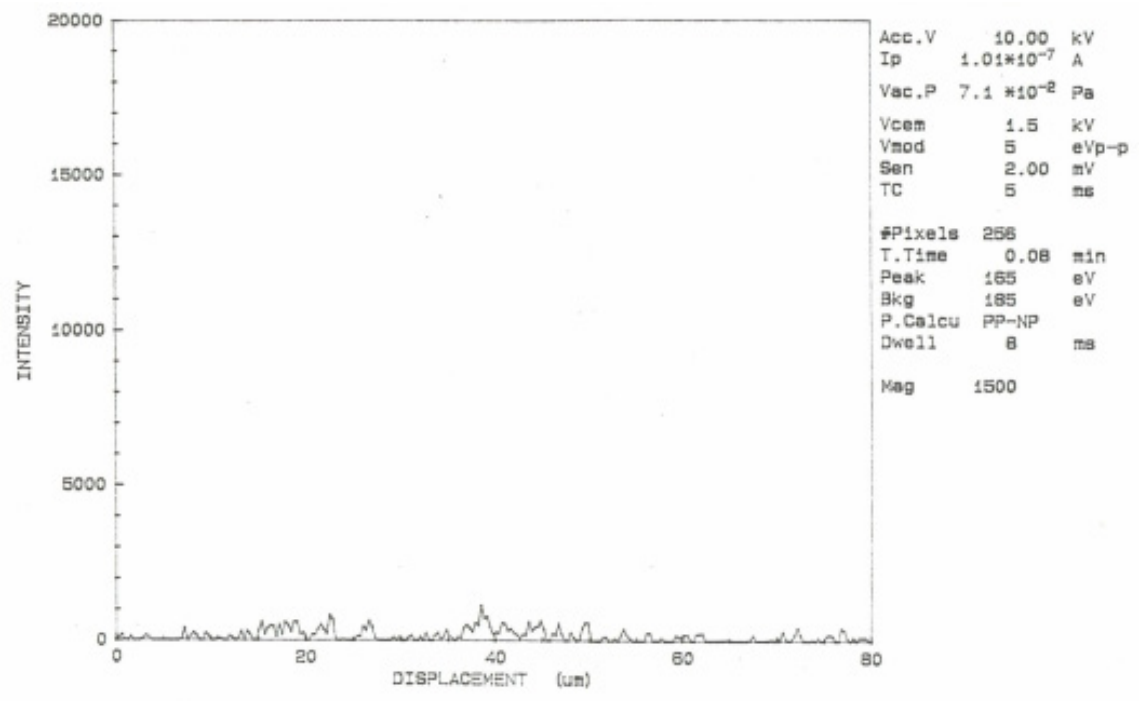

Figure 3. AES Line scan showing B peaks at different locations

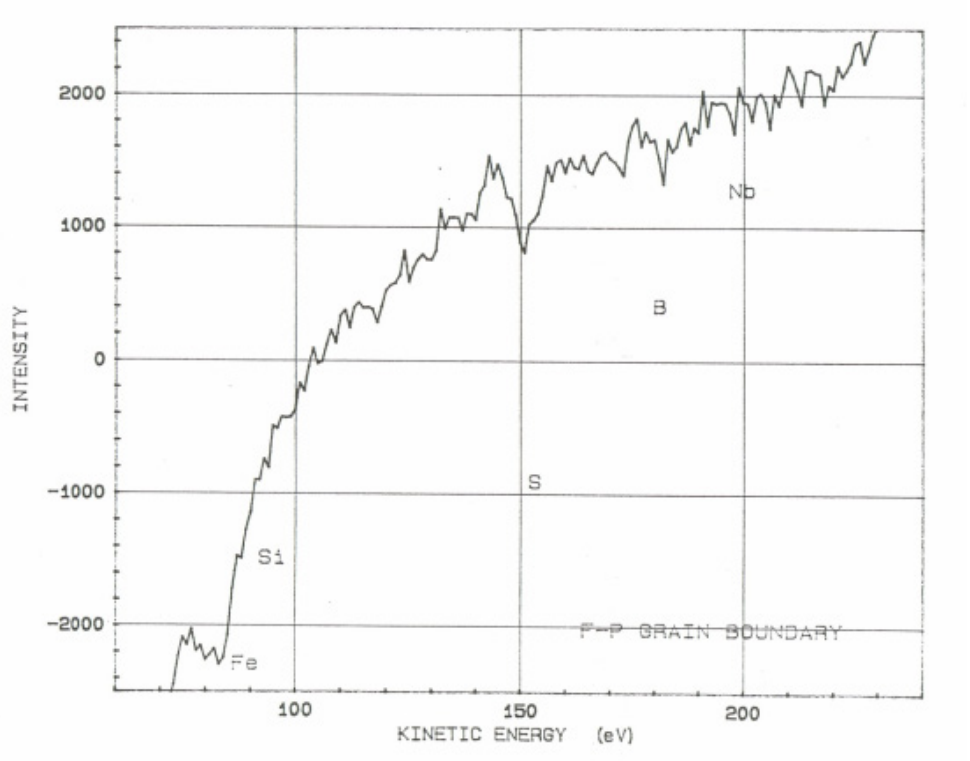

Figure 4. AES point analysis showing B peaks at ferrite-pearlite grain boundary

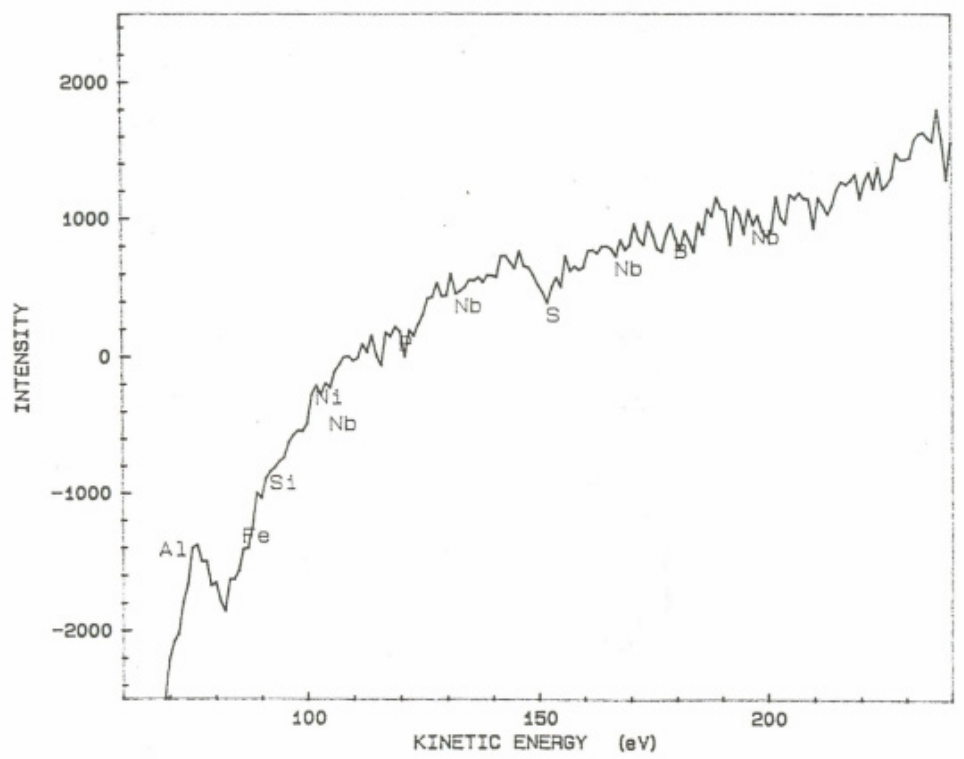

Figure 5. AES point analysis showing no B peak within ferrite grain

4.3. Thermal Analyses

Studies on thermal analyses of microalloyed steel comprised an assessment of critical/ transformation temperatures through differential thermal analysis, and calculation of enthalpy of transformations. DTA versus temperature plots along with DDTA are depicted in Fig. 6. The results obtained on analysing the data are presented below:

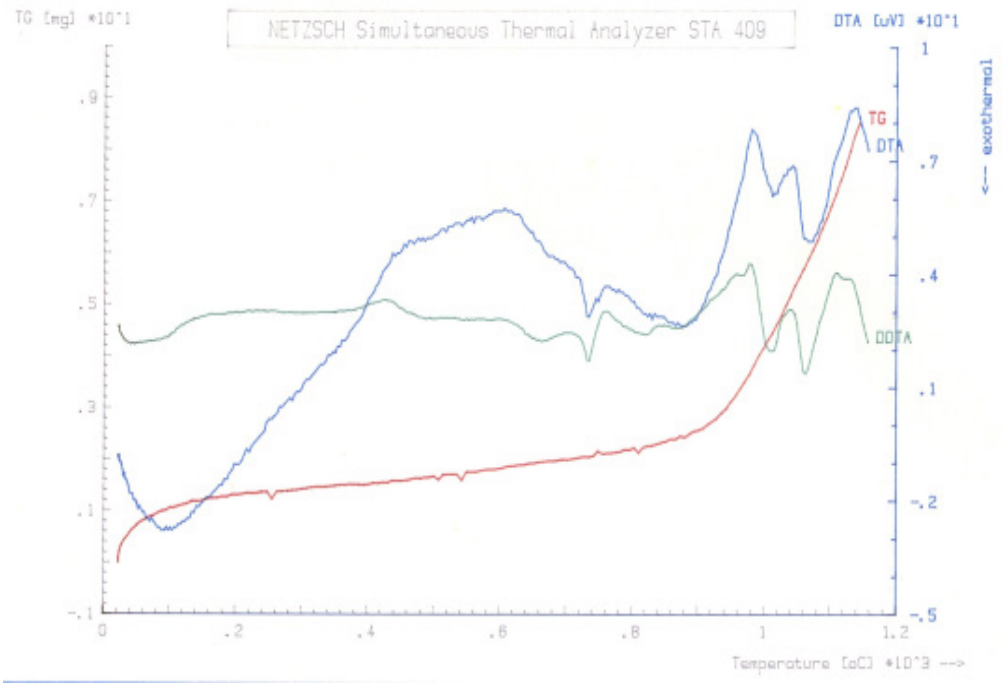

Figure 6. DTA and DDTA plots showing transformation temperatures

4.4. Critical/Transformation Temperatures

i) First deviation in the DTA curve, was observed at 430°C. This, most probably, corresponds to relaxation of stresses introduced during machining of the specimen to powder form. The said process apparently got completed by ~610°C.

ii) First phase transformation took place at 715°C which is close to the ferrite→austenite transformation start temperature (Ac_1:713°C) as calculated empirically. The transformation reached to its peak at 734°C followed by pearlite→austenite transformation at 745*C. Subsequently, this trans-formation got completed at ~768°C. Between 715-768°C, with a peak at 734°C, the enthalpy (ΔH) of the transformation and latent heat (ΔC_p) were estimated as -9.4 J/g and -0.232 J/g°K, respectively. The negative values of ΔH and ΔC_p indicated that ferrite to austenite and cementite to austenite transformations are exothermic in nature.

iii) Second transformation was observed between 980-1044°C with a peak at 1014°C. Enthalpy and latent heat calculated for this peak were -48.6 J/g and -0.583 J/g°K, respectively. This exothermic energy was liberated, in all probability, due to the dissolution of $M_{23}(C,B)_6$ precipitate in the aforementioned temperature range[7,8].

iv) The above transformation was followed by another transformation between 1044°-1140°C. Enthalpy and latent heat, calculated for a peak at 1074°C, were found to be -58.4 J/g and -0.692 J/g°K, respectively. The energy values, thus attained in all probabilities represent the dissolution of NbC precipitate into austenite[7,8].

5. Discussion

The microstructure of the material in the hot rolled condition followed by air cooling comprised ferrite+ degenerated pearlite with an average ferrite grain size of ~12 μm. The important feature is definitely the presence of degenerated pearlite. It is evident that its formation has been largely brought about by the presence of boron. This observation is based on the premise that in an equivalent B-free steel, no degenerated pearlite forms. It would therefore be necessary to arrive at an indepth understanding of the effect of Nb & B both individually and when acting in tandem on the overall transformation behaviour of the steel under investigation. Without going into details, it would not be out of place to suggest that the formation of degenerated pearlite is perhaps an out come of; i) the likelihood of forming bainite type structure at relatively faster cooling rates due to the presence of B, and ii) the likely effect of Nb & B in influencing the carbide formation step constituting pearlite.

During reheating of the billets at 1200°C, for 1-1½ hours, carbides and other similar compounds mostly dissolve, thereby ensuring that alloying elements such as Nb, B, Al, C go into solution. In so far as the solubility of these elements at high temperatures is concerned, it mainly depends upon the atomic size and the affinity amongst interacting species. Empirical relationships exist for computing solubility at a given heat treating temperature. For the experimental steel, the amount of Nb dissolved in equilibrium with C, could be calculated by using the relationship[9] :

$$\log[\,Nb\%\,][\,C\%\,] = -7900/T + 3.42.$$

On substituting for C (as 0.13%), ~0.088% Nb could be dissolved at 1473°K. Irvine et al. indicated that N also contributes to carbon equivalence. For such steels (C:N>10) they proposed the relationship:

$$\log[Nb][C + 12\,N/14] = -6770/T + 2.26$$

Since the experimental steel contains C and N in the ratio of ~18.57, the amount of soluble Nb that can be accommodated in equilibrium with 0.13%C and 70 ppm N at 1473°K is ~0.034%. The amounts of Nb calculated through the aforementioned relations, namely 0.088 & 0.034%, are higher than the one present in the experimental steel (0.023%). It would not be incorrect to infer, therefore, that most of the Nb present in the experimental steel is in the dissolved state on reheating the billets at 1200°C.

It would now be pertinent to examine the effect of Nb and other alloying elements in influencing the processing schedule. While little effect has been observed on reheating at 1200°C, ease of deformation is influenced at lower temperatures[10]. During hot deformation, excess dislocations being generated anneal out, thereby leading to the attainment of a sub-grain structure. At rolling temperatures of 1050-1150°C, in combination with larger strains generated due to higher speed of rolling, critical strain is easily reached and this causes austenite to recrystallise. In roughing stands of wire rod mill rolling speed is comparatively low but temperature of about 1150°C is good enough for inducing recrystallisation. Similarly, at the finishing stage, despite the temperature being lower (1075°C), higher strains generated due to higher rolling speeds induce recrystallisation to occur.

The occurrence of recrystallisation during hot working is thus a fundamental happening. Presence of alloying elements would, however, influence the recrystallisation kinetics of austenite and it is quite likely that under certain conditions it may not go to completion. The presence of alloying elements, in general, raises the recrystallisation temperature. Nb and B are known to influence it markedly through their precipitate forming tendency and the resultant well known pinning and solute drag effects. In order that maximum benefits are derived from these effects, it would be most useful to have Nb and B in solution before starting rolling. This is important because the basic condition for obtaining grain refinement during processing is that reprecipitation of the grain refining precipitates (in the present instance Nb bearing compounds) and recovery/ recrystallisation should occur simultaneously.

The mechanism suggested envisages that as rolling is initiated, the fibered structure formed due to deformation recovers/ recrystallises. At the same time reprecipitation of the Nb bearing compounds begins, perhaps on the sub-grain boundaries formed due to recovery. This is useful in pinning sub-boundaries. As the number of passes increase the aforementioned steps are repeated. Despite a likely fall in

temperature as the rolling proceeds, the Nb bearing precipitates coarsen since the absolute value of temperature is high. The precipitate in its coarsened form is useful in restricting grain boundary migration. By the time the temperature reaches 950-1000°C most of the grain boundaries/ sub-boundaries are expected to be pinned and as such it is most useful to terminate rolling at this stage. Consequently it would be possible to retain the microstructure attained at the finishing stage down to room temperature without the necessity of having to alter the cooling rate. Thus, it is clear that the fraction of Nb that has separated as a precipitate in austenite is contributing to grain refining during controlled processing.

Regarding the nature of the precipitating Nb compounds, Nordberg and Aaronson[11] have demonstrated through thermodynamical calculations that it forms NbC rather than Nb(C,N) in the alloys containing C:N≥5. In the material under study the ratio happens to be ~19. Therefore, presence of Nb in the form of NbC was most probable. Moreover, since C in solution was surplus, the amount left over after combining with Nb, could be effectively fixed with boron. Studies[8,12] have revealed that if C and B are present in solution near Ac_3 temperature they combine and form $M_{23}(C,B)_6$ type of precipitates at austenite grain boundaries and grain interiors. Since Nb has already been fixed as NbC, iron atoms are thermodynamically the next option to adopt the atomic configuration of $M_{23}(C,B)_6$. Therefore, $M_{23}(C,B)_6$ is the favoured precipitate to consume the available boron. Since Nb is effectively consumed in forming NbC, it is no longer effective in suppressing the $\gamma \rightarrow \alpha$ transformation. Therefore, on cooling at slower rate of about 1°C/sec, as used in industrial wire rod mills, lower transformation products such as bainite and martensite did not form since neither Nb nor B is able to contribute to such an happening. At such a low cooling rate ferrite did not experience much resistance to nucleate at austenite grain boundaries and other imperfections. Due to its low solubility in ferrite, carbon was rejected during ferrite grain growth and this finally resulted into the formation of pearlitic microstructure. It is interesting to note that inspite of low cooling rate in the wire rod mill, formation of lamellar morphology of carbides (cementite) could be avoided. This was made possible due to the synergistic effect of Nb and B, exerted on the kinetics of $\gamma \rightarrow \alpha$ phase transformation. The non-lamellar morphology of degenerated pearlite is some what similar to that of acicular ferrite having broken chains of cementite inside ferrite matrix. As suggested in the literature acicular ferrite has also been described as a form of upper bainite. It may, therefore, be appropriate to mention that degenerated pearlite is a microstructure which has its characteristics between lamellar pearlite and upper bainite and hence, in terms of properties, is expected to perform better than lamellar carbides. In the light of the above mentioned analysis the properties of the as rolled material appear to be reasonable with total elongation and reduction in area values better than what can be normally expected.

It is known that on cooling the recrystallised austenite from finishing temperatures of about 950-1000°C to room temperature compounds of Al, N, Nb, B, C etc. start precipitating out after the $\gamma \rightarrow \alpha$ transformation. The extent of precipitation depends upon their volume fraction, affinity towards each other and solubility in α (which is negligible). As far as N is concerned, it forms AlN rather than BN if Al:N exceeds the stoichiometric ratio of 1.93[8,13,14]. In the experimental alloy, therefore, precipitation of AlN was expected since Al:N ratio was about 5.7. Similarly, Nb will precipitate as NbC and along with AlN will precipitation harden ferrite. Coming to the role of boron, Cameron and Morral[15] have reported that the solubility of B in austenite and ferrite phases is extremely small as based on the Fe-C-B system. On the other hand, cementite can take up a large amount of B as a substitute for carbon forming $Fe_3(C,B)$ precipitates consisting of Fe_3C and Fe_3B components. Perez et al.[14,16] detected three types of boron precipitates through high resolution electron microscopy. These precipitates are FeB, $M_{23}(C,B)_6$ and B_4C type in boron microalloyed steel. The aforementioned information is likely to prove useful in deciding how B would be distributed in the experimental material.

A study of the relevent portion of the Fe-C-B diagram revealed that for a composition containing 0.13 wt.% carbon and 10 ppm B precipitation of $M_{23}(C,B)_6$ occurred in the temperature range ~740-770°C[16]. It was further proposed by Watanabe et al.[8,16] that precipitation of $M_{23}(C,B)_6$ mostly takes place between Ac_3 and Ac_1 temperatures. For the experimental steel they are 839°C and 713°C, respectively and within this temperature range only about 10 ppm boron would participate in the formation of $M_{23}(C,B)_6$. Evidently, most of it (~30 ppm) is likely to precipitate with cementite in the form of boron containing compounds such as $FeB/Fe_2B/B_4C$ or a combination of these during $\gamma \rightarrow \alpha$+pearlite transformation. This perhaps accounts for the formation of boron rich regions inside pearlitic colonies and comparatively, lower density of $M_{23}(C,B)_6$ precipitates at ferrite grain boundaries at slower cooling rates (Figs. 2a & b). As the cooling rate is raised a part of this 30 ppm boron will effectively contribute towards the formation of intermediate or lower temperature transformation products.

Having thus explained B segregation at the boundaries and reasons for its presence in larger amounts within the pearlitic regions, it is now necessary to comment upon its presence/ segregation at the ferrite-pearlite interface and its absence inside ferrite grains. The former is consistent with the general understanding that boron would be found in close proximity of the carbide phase. The latter observation agrees well with the known tendency of B to segregate to prior boundaries.

Despite a relatively lower Nb content, the ferrite grain size obtained in the as hot rolled condition (~ASTM;9) is comparable to that obtained in microalloyed HSLA steel. This is perhaps on account of the presence of Al (0.04%) which may be contributing to grain refining/ precipitation hardening due to the formation of AlN. A yet another aspect which could have contributed indirectly is the Nb-B

synergism, thereby facilitating the fixing up of extra carbon (beyond that which combines with 0.023% Nb).

It is well understood that for attaining desired properties in steels transformation temperatures and cooling rate play an important role since they ultimately control the end microstructure in materials. Accurate measurement of these parameters is, therefore, necessary. For this reason, transformation temperatures were calculated for the chemistry using Andrews[6] empirical relations and confirmed through differential thermal analysis. This validates the relevance of the empirical formulations and justifies calculation of temperatures such as M_s, M_f etc. using them.

The aforementioned critical/ transformation temperatures alone did not fully reveal the transformations occuring in the experimental material. DTA, besides helping in ascertaining the additional information, was also useful in confirming either fully or partly the information thus far obtained. It was revealed that the energy peaks at ~1014°C and 1074°C (latent heats of about -0.583 j/g°K and about -0.692 j/g °K, respectively) denoted dissolution/ precipitation of $Fe_{23}(C,B)_6$ and NbC precipitates[7,8], respectively. Thus DTA proved helpful in arriving at a more detailed understanding of the transformation behaviour as it was able to detect transformations not discernible with the help of dilatometry.

On analysing tensile results it was revealed that above referred microstructures helped in attaining a total elongation of 35%, uniform elongation of 17% and reduction in area of 70% in the experimental steel. The high value of elongation along with large reduction in area values indicated that the steel is adequately formable for sustaining large deformations imparted during cold heading operations carried out while forming the components.

6. Conclusions

Based upon the results obtained through optical microscopy, Auger electron spectroscopy and differential thermal analysis and subsequent discussions thereon, following inferences may be arrived at:

1. In as rolled condition the wire rods contained about 12 to 15 % degenerate pearlite the balance being polygonal ferrite. The average ferrite grain size was found to be ~12 μm.

2. Auger electron spectroscopy revealed that B was segregated within pearlitic colonies as well as at the grain boundaries. Through DTA analysis and enthalpy calculations it emerged that B is likely to be present as $M_{23}(C,B)_6$.

3. Nb was found to be distributed throughout the matrix, most likely as NbC.

ACKNOWLEDGEMENTS

Authors are thankful to the management of RDCIS for permitting presentation of this paper in the international conference SIMPRO'2012.

REFERENCES

[1] R. Herschitz and D.N. Seidman, Acta Met. 33, 1547 (1985).

[2] M.J. Luton, R. Dorvel and R.A. Petkovic, Met. Trans., 11A, 411 (1980).

[3] X.L. He, M. Djahazi, J.J. Jonas and Jackman, Acta Met., Vol. 39, No. 10 (1991), P. 2295.

[4] H. Tomehiro, M. Murata, R. Habu and M. Naguma, Trans. ISIJ 27, (1987), P. 120.

[5] Auger Electron Specroscope Manual.

[6] KW Andrews, JISI, July 1965, P.721.

[7] S. Watanabe et al., Trans. ISIJ,Vol.23, (1983), P.31.

[8] S. Watanabe and H. Ohtani, Trans. ISIJ, Vol.23, (1983), P.38.

[9] K.J. Irvine, F.B. Pickering and T. Gladman, JISI, 205, (1967), P. 161.

[10] D.Zhang, A.J. Baker and P.R. beeley, Material Science and Technology, Vol.10, Oct (1994), P.903.

[11] H. Nordberg and B. Aronsson, JISI, 206, (1968), P. 1263.

[12] Y. Omori, Trans. ISIJ, No.11, P.339.

[13] S. Watanabe, H. Ohtani and T. Kunitake, Trans. ISIJ, Vol.23, (1983), P.121.

[14] K. Sugimoto et al., Trans. ISIJ, Vol.26, (1986), P.329.

[15] T.B. Cameron and J.E. Morall, Met. Trans., Vol.17A, Aug. (1986), P.1481.

[16] R. Perez, A. Garcia and J.A. Jaurez, Scripta Met., Vol.28, (1993), P931.